

International Journal of Modern Physics E
 © World Scientific Publishing Company

GLOBAL NUCLEAR STRUCTURE ASPECTS OF TENSOR INTERACTION

W. SATUŁA^{a),b)*}, M. ZALEWSKI^{a)}, J. DOBACZEWSKI^{a),c)}, P. OLBRATOWSKI^{a)},
 M. RAFALSKI^{a)}, T.R. WERNER^{a)}, and R.A. WYSS^{b)}

^{a)}*Institute of Theoretical Physics, University of Warsaw, ul. Hoża 69, 00-681 Warsaw, Poland*

^{b)}*KTH (Royal Institute of Technology), AlbaNova University Center, 106 91 Stockholm, Sweden*

^{c)}*Department of Physics, P.O. Box 35 (YFL), FI-40014 University of Jyväskylä, Finland*

Received (received date)

Revised (revised date)

A direct fit of the isoscalar spin-orbit and both isoscalar and isovector tensor coupling constants to the $f_{5/2} - f_{7/2}$ SO splittings in ^{40}Ca , ^{56}Ni , and ^{48}Ca requires (*i*) a significant reduction of the standard isoscalar spin-orbit strength and (*ii*) strong attractive tensor coupling constants. The aim of this paper is to address the consequences of these strong attractive tensor and weak spin-orbit fields on total binding energies, two-neutron separation energies and nuclear deformability.

1. Introduction

Density functional theory (DFT) is a method of choice in large-scale calculations of nuclear properties. In spite of certain difficulties related to rigorous formulation of the DFT for self-bound systems like atomic nuclei, the method is potentially exact, which is guaranteed by the Hohenberg-Kohn-Scham (HKS) theorems^{1,2}, see recent discussion in Refs.^{3,4,5}.

Due to the complexity of nuclear many-body problem in general, and of the effective nucleon-nucleon interaction in particular, there exist no universal rules for constructing nuclear energy density functional (EDF). In this respect, our intuition is almost solely based on symmetry properties and practical knowledge, accumulated over the years for density-dependent effective interactions of Skyrme⁶ or Gogny⁷ type being applied within the mean-field (MF) approximation. Free parameters of these interactions or functionals are fitted to empirical data. Hence, the quality and performance of these methods strongly depends on adopted fitting strategies and datasets⁸.

Conventional fitting methods use datasets that are dominated by bulk nuclear matter data and by nuclear binding energies of selected double-magic nuclei, with essentially no data on the single-particle (s.p.) energies. Such strategies have quite

*satula@fuw.edu.pl

2 *W. Satuła, J. Dobaczewski, P. Olbratowski, M. Rafalski, T.R. Werner, R.A. Wyss, and M. Zalewski*

dramatic consequences concerning mostly spin-orbit (SO) and tensor parts of the EDF. In particular, they lead to an artificial isoscalar-effective-mass scaling of the SO strengths⁹, contradicting scaling in selected s.p. splittings¹⁰, and perpetual problems in reproducing evolution of the proton (neutron) s.p. energy splittings versus the neutron (proton) shell filling along the isotopic or isotonic chains of nuclei.

The most prominent examples of such chains include: neutron-rich oxygen¹¹, neon¹², sodium^{13,14}, magnesium¹⁵, titanium^{16,17}, or, in medium-mass region, antimony¹⁸ isotopes. In fact, a non-conventional shell evolution found in these neutron-rich nuclei directly motivated the shell-model theorists to introduce the so-called monopole shifts, to account for empirical trends. The physical origin of these shifts was, in turn, attributed to the shell-model tensor interaction^{19,20,21}. Connection between the monopole-shifts and the tensor interaction was later on confirmed within the self-consistent MF models using either finite-range Gogny force²² or contact Skyrme interaction^{23,24,25,26,27,28,29} augmented by a strong tensor interaction.

Single-particle spectra provide for a clear evidence of strong tensor interaction and call for a new strategy of fitting the nuclear EDF in general, and of the SO and tensor terms in particular, directly to the s.p. data^{28,30}. The use of the s.p. levels was usually contested, because of the isoscalar-effective-mass scaling (m^*) of s.p. levels. Several authors^{31,32,33} argued that the physical density of s.p. levels around the Fermi energy can be reinstated only after the inclusion of particle-vibration coupling, that is, by going beyond MF. In our opinion, effective EDF theories should warrant a proper value of the effective mass through the fit to empirical data and readjust other coupling constants to this particular value of m^* , leading to fairly m^* independent predictions. Hence, fitting strategies can include information on s.p. levels provided that the s.p. levels are understood through the binding-energy differences between doubly-magic cores and the lowest s.p. states in odd- A single-particle/hole neighbors^{34,28}. Spherical s.p. energies or, more precisely, the Kohn-Sham s.p. energies computed in even-even double-magic core should serve only as auxiliary quantities.

In our recent study²⁸, we have proposed a novel fitting strategy of the SO and tensor terms in the nuclear EDF. It is based on a direct fit to the $f_{7/2} - f_{5/2}$ SO splittings in spin-saturated isoscalar nucleus ^{40}Ca , spin-unsaturated isoscalar nucleus ^{56}Ni , and spin-unsaturated isovector nucleus ^{48}Ca . The procedure allows for fixing three out of four coupling constants in this sector, namely, the isoscalar strengths of the SO and tensor interactions and the ratio of the isovector coupling constants. The procedure indicates a clear need for a major reduction of the SO strength and for strong attractive tensor fields. The aim of the present work is to address further consequences of strong attractive tensor and weak SO fields on binding energies, two-neutron separation energies, and nuclear deformability.

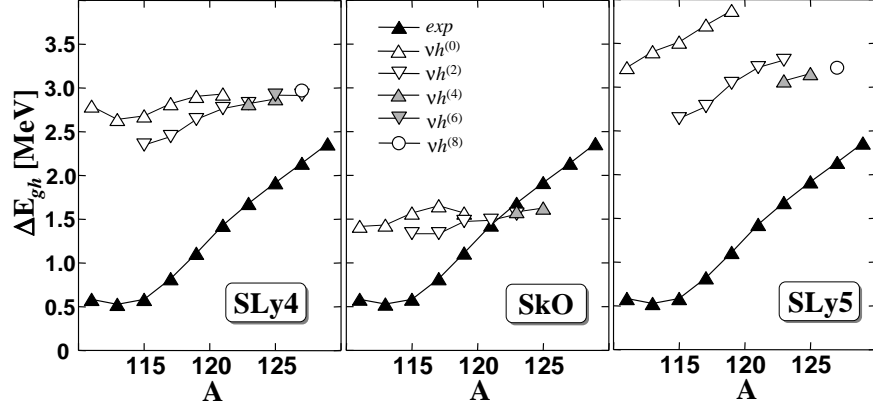


Fig. 1. The $\pi h_{11/2} - \pi g_{7/2}$ splitting in ${}_{51}^A\text{Sn}$ isotopes versus A . Black triangles label empirical data taken from Ref. 18. Open and gray symbols represent the SHF results obtained by using the SLy4 (left) SkO (middle), and SLy5 (right) parameterizations, respectively. Different symbols labeling theoretical results follow the SHF minima corresponding to configurations differing in the $\nu h_{11/2}$ occupancies as indicated in the legend.

2. Fitting the tensor strengths to single-particle energies

The s.p. levels constitute one of the main building blocks of the MF method. In spite of that, the Skyrme HF (SHF) method that uses forces fitted to bulk nuclear properties performs rather poorly with regard to the s.p. SO splittings^{28,30}. This is visualized in Fig. 1, showing the $\pi 1h_{11/2} - \pi 1g_{7/2}$ splittings, ΔE_{gh} , in antimony, calculated by using the SLy4³⁵, SkO³⁶, and SLy5³⁵ parameterizations. The SLy4 force strongly overestimates the absolute value of ΔE_{gh} and fails to reproduce the slope of the $\Delta E_{gh}(A)$ curve. The non-standard isovector SO in the SkO force helps by reducing, on average, the splitting to the empirical level, but does not change the slope of the $\Delta E_{gh}(A)$ curve. Finally, in SLy5, the inclusion of tensor terms changes the slope, but shifts the theoretical curves in a wrong direction. The latter observation suggests that the fit to masses leads to values of tensor coupling constants that are at variance with those deduced from the s.p. level analysis, see Refs.^{37,28}. However, one should point out that the $\pi 1h_{11/2} - \pi 1g_{7/2}$ splittings depend upon many factors including, apart from the SO and tensor fields, the effective mass, centroid energies of the $\ell = 4$ and $\ell = 5$ sub-shells, and strong polarization effects. Hence, conclusions concerning the SO and tensor coupling constants that are deduced solely from these data should be considered to be tentative.

It is well known, see Refs.^{41,42}, that the tensor interaction strongly modifies the SO one-body potential. In the spherical-symmetry limit, the isoscalar ($t = 0$)

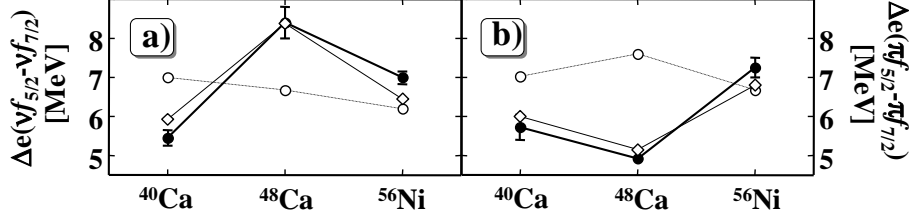
4 *W. Satuła, J. Dobaczewski, P. Olbratowski, M. Rafalski, T.R. Werner, R.A. Wyss, and M. Zalewski*

Fig. 2. The neutron (top) and proton (bottom) $1f_{7/2} - 1f_{5/2}$ SO splittings in ^{40}Ca , ^{48}Ca , and ^{56}Ni . Black symbols show the mean empirical values taken from Refs.^{38,39} and open dots denote the SkO results. Open diamonds represent the results obtained by using the SkO $_{T'}$ functional of Ref.⁴⁰, which includes strong attractive tensor terms and a reduced SO strength.

and isovector ($t = 1$) SO one-body potentials read:

$$W_t^{SO} = \frac{1}{2r} \left(C_t^J J_t(r) - C_t^{\nabla J} \frac{d\rho_t}{dr} \right) \mathbf{L} \cdot \mathbf{S}, \quad (1)$$

where C_t^J and $C_t^{\nabla J}$ are the tensorial and spin-orbit coupling constants, see for example Ref.²⁸. The tensor field depends upon the radial component of the spin-orbit vector density $\mathbf{J}_t = \frac{r}{r} J_t(r)$ that measures the spin-asymmetry of the nucleus and can rapidly vary with particle numbers. On the contrary, the second term in Eq. (1), which is due to the conventional two-body spin-orbit interaction, depends on the radial derivative of the particle density ρ_t , which varies relatively slowly with particle numbers. Such a contrasting behavior of the two major constituents of the SO potential can be actually used to fit the coupling constants to data²⁸. The idea is visualized in Fig. 2, which shows the $1f_{7/2} - 1f_{5/2}$ SO splittings in ^{40}Ca , ^{48}Ca , and ^{56}Ni . These splittings form a very distinct pattern that cannot be reproduced based solely on the conventional SO potential. Indeed, the $1f_{7/2} - 1f_{5/2}$ SO splittings in ^{40}Ca , ^{48}Ca , and ^{56}Ni are fairly constant when calculated using, for example the SkO force, see curve marked by open dots in Fig. 2. It reflects the fact that the neutron and proton radial form-factors $\frac{d\rho}{dr}$ almost do not change when going from ^{40}Ca through ^{48}Ca to ^{56}Ni . At the same time the neutron and proton SO vector densities $J(r)$ change rapidly when going from the isoscalar spin-saturated ^{40}Ca to the isoscalar spin-unsaturated nucleus ^{56}Ni , and, finally, to the isovector spin-unsaturated nucleus ^{48}Ca . This allows for a simple and intuitive three-step fitting procedure²⁸ of the $C_0^{\nabla J}$ in ^{40}Ca , C_0^J in ^{56}Ni , and $C_1^J/C_1^{\nabla J}$ ratio in ^{48}Ca . This procedure leads to (i) a significant reduction in the isoscalar SO strength and (ii) strong attractive tensor coupling constants. It systematically improves such s.p. properties as the SO splittings and magic-gap energies²⁸, but leads to deteriorated nuclear binding energies.

3. Tensor interaction and the nuclear binding energies

As discussed in Ref.⁴³, the tensor contribution to the nuclear binding energy shows interesting generic topological patterns closely resembling those of the shell-

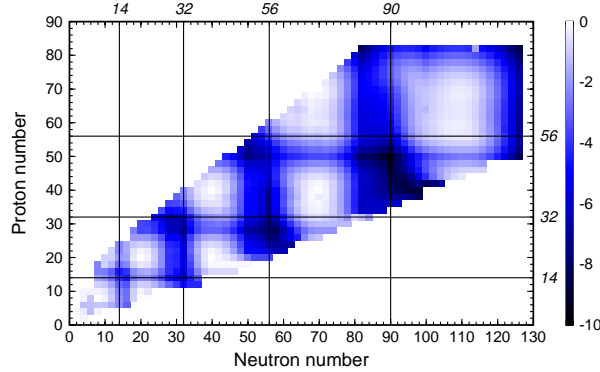


Fig. 3. Tensor contributions to the total binding energy calculated by using the spherical Hartree-Fock-Bogoliubov model with the $SLy4_T$ functional of Ref.²⁸. Vertical and horizontal lines indicate the tensorial magic numbers. From Ref.⁴³.

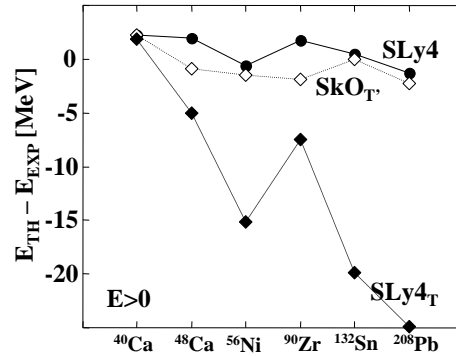


Fig. 4. Differences between theoretical and experimental binding energies (positive) in selected double-magic nuclei. Black dots represent the results obtained using conventional $SLy4$ force. Black and white diamonds label the results calculated using the $SLy4_T$ and the $SkO_{T'}$ functionals, respectively.

correction, see Fig. 3. The single-particle *tensorial magic numbers* at $N(Z)=14, 32, 56, \text{ or } 90$, corresponding to the maximum spin-asymmetry in the $1d_{5/2}, 1f_{7/2} \oplus 2p_{3/2}, 1g_{9/2} \oplus 2d_{5/2}$ and $1h_{11/2} \oplus 2f_{7/2}$ spherical s.p. configurations, respectively, are clearly seen in the figure. Note, that the calculated tensorial magic numbers are shifted due to configuration mixing toward the classic magic numbers of $N(Z)=8, 20, 28, 50, \text{ and } 82$. The topological features shown in Fig. 3 are fairly independent of a specific parameterization of the force. Indeed, they simply reflect the order of s.p. levels, which is rather unambiguously established and relatively well reproduced by the state-of-the art nuclear MF models, at least in light and medium-mass nuclei.

Values of the tensor and SO strengths deduced from the s.p. properties are at variance with those obtained from mass fits^{37,40}. A large reduction of the SO

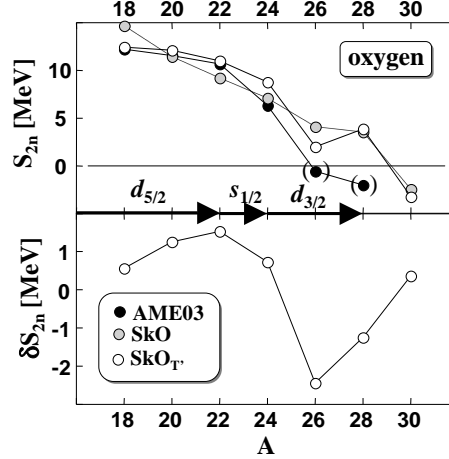
6 *W. Satuła, J. Dobaczewski, P. Olbratowski, M. Rafalski, T.R. Werner, R.A. Wyss, and M. Zalewski*

Fig. 5. Two-neutron separation energy S_{2n} (upper part) in oxygen isotopes. Empirical data ⁴⁴ are labeled by black dots. Theoretical values obtained using the SkO and SkO_{T'} functionals are marked by gray and white dots, respectively. Lower part shows contribution of the tensor term to the S_{2n} as a function of shell filling.

strength, which is particularly strong for the low- m^* forces like SLy4, has a particularly destructive impact on theoretical binding energies, see Fig. 4.

A multidimensional fit to masses shows that the mass performance of the SLy4_T force can be improved by a tiny refinements of the remaining coupling constants²⁸, however, the accuracy of the original SLy4 cannot be regained. This indicates that a *spectroscopic quality* parameterization that would perform reasonably well on binding energies must have large effective mass, $m^* \geq 0.9$. One of the candidates is the SkO_{T'} functional of Ref.⁴⁰. This functional, at least for the classical set of double-magic nuclei shown in Fig. 4, is of a similar accuracy as SLy4, and it outperforms both the SLy4_T and SLy4_{Tmin} of Ref.²⁸.

This allows for reasonable quantitative estimates of the tensor influence, for example, on two-neutron separation energies, potential energy surfaces (PES's), and onset of deformation. An example of calculation of the two-neutron separation energies for oxygen nuclei is shown in Fig. 5. One clearly sees here the way the tensor interaction induces in oxygen isotopes a breaking of stability against the two-neutron emission around ²⁶O. Indeed, as shown in the lower panel of the figure, in ²⁶O a decrease of S_{2n} is directly related to the $d_{3/2}$ sub-shell occupation that reduces the spin-asymmetry and tensor contribution to the binding energy.

By deforming the nucleus one can easily change the spin asymmetry and, in turn, tensor effects. Fig. 6 shows the PES's versus quadrupole deformation in ⁸⁰Zr (left) and ¹²⁰Sn (right), calculated by using the quadrupole-constrained HFB method. At the spherical shape, nucleus ⁸⁰Zr is spin-saturated. By deforming the system, one increases the spin-asymmetry by enforcing the occupation of the $g_{9/2}$ sub-shell. By adding to SkO a strong attractive tensor field (SkO_{TX}), one pulls the

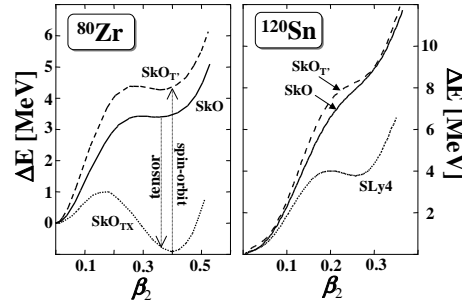


Fig. 6. Potential energies versus axial quadrupole deformation parameter β_2 in ^{80}Zr (left) and ^{120}Sn (right), calculated by using the SkO, SkO_{TX}, SkO_{T'}, and SLy4 functionals. See text for details.

deformed minimum down. The consecutive reduction of the SO strength (SkO_{T'}) provides for a compensation mechanism, and it shifts the $g_{9/2}$ sub-shell and the deformed minimum up in energy, back to its original position obtained for the SkO functional. In ^{56}Ni , a similar compensation mechanism is found in the yrast super-deformed bands, see Ref.⁴⁰. In case of ^{120}Sn , the PES's calculated by using the SkO and SkO_{T'} parameterizations are again very close to each other. Note however, that both these curves differ substantially from the PES calculated using the SLy4 parameterization.

4. Summary

In this study, we discussed specific nuclear-structure effects induced by strong attractive tensor fields and weak spin-orbit field, which result from direct fits of the coupling constants to the SO splittings. In particular, we showed that contributions to the nuclear binding energies that are due to the tensor field show a generic *magic structure* with *tensorial magic numbers* at $N(Z)=14, 32, 56, \text{ or } 90$ corresponding to maximum spin-asymmetry in $1d_{5/2}, 1f_{7/2} \oplus 2p_{3/2}, 1g_{9/2} \oplus 2d_{5/2}$ and $1h_{11/2} \oplus 2f_{7/2}$ single-particle configurations. We also demonstrated that it is possible to construct a functional being able to simultaneously reproduce the $f_{5/2} - f_{7/2}$ SO splittings in ^{40}Ca , ^{56}Ni , and ^{48}Ca nuclei and binding energies of doubly magic spherical nuclei. By using this particular functional, we discussed specific structural effects, pertaining to strong tensor terms, exerted on two-neutron separation energies in oxygen isotopes and PES's in ^{80}Zr and ^{120}Sn . In particular, in the context of nuclear deformation properties, we discussed compensation mechanism between the attractive tensor fields and weak SO field.

This work was supported in part by the Polish Ministry of Science under Contract No. N N202 328234, by the Academy of Finland and University of Jyväskylä within the FIDIPRO programme, and by the Swedish Research Council.

8 *W. Satuła, J. Dobaczewski, P. Olbratowski, M. Rafalski, T.R. Werner, R.A. Wyss, and M. Zalewski*

References

1. P. Hohenberg and W. Kohn, Phys. Rev. **136**, B864 (1964); M. Levy. Proc. Nat. Acad. Sci. **76**, 6062 (1979).
2. W. Kohn and L.J. Sham, Phys. Rev. **140**, A1133 (1965).
3. J. Engel, Phys. Rev. C **75**, 014306 (2007).
4. B.G. Giraud, Phys. Rev. **C77**, 014311 (2008).
5. B.G. Giraud, B.K. Jennings, and B.R. Barrett, Phys. Rev. **A78**, 032507 (2008).
6. T.H.R. Skyrme, Phil. Mag. **1** (1956) 1043; Nucl. Phys. **9** (1959) 615.
7. D. Gogny, Nucl. Phys. **A237**, 399 (1975).
8. P. Klüpfel, P.-G. Reinhard, J. A. Maruhn, arXiv:0804.3402.
9. H. Zduńczuk *et al.*, Phys. Rev. **C71**, 024305 (2005); Int. J. Mod. Phys. **E14**, 451 (2005) .
10. W. Satuła, R.A. Wyss and M. Zalewski, Phys. Rev. **78**, 011302(R) (2008).
11. E. Becheva *et al.*, Phys. Rev. Lett. **96**, 012501 (2006).
12. M. Bellegruic *et al.*, Phys. Rev. **C72**, 054316 (2005).
13. Y. Utsuno *et al.*, Phys. Rev. **C70**, 044307 (2004).
14. V. Tripathi *et al.*, Phys. Rev. Lett. **94**, 162501 (2005).
15. G. Neyens *et al.*, Phys. Rev. Lett. **94**, 022501 (2005).
16. B. Fornal *et al.*, Phys. Rev. **C70**, 064304 (2004).
17. D.-C. Dinca *et al.*, Phys. Rev. **C71**, 041302 (2005).
18. J.P. Schiffer *et al.*, Phys. Rev. Lett. **92**, 162501 (2004).
19. T. Otsuka *et al.*, Phys. Rev. Lett. **87**, 082502 (2001).
20. T. Otsuka *et al.*, Phys. Rev. Lett. **95**, 232502 (2005).
21. M. Honma *et al.*, Eur. Phys. Jour. **25**, s01, 499 (2005).
22. T. Otsuka, T. Matsuo, and D. Abe, Phys. Rev. Lett. **97**, 162501 (2006).
23. J. Dobaczewski, in Proceedings of the *Third ANL/MSU/INT/JINA RIA Theory Workshop: Opportunities with Exotic Beams*, Argonne, IL, April 4-7, 2006, eds. T. Duguet, H. Esbensen, K. M. Nollet, and C. D. Roberts (World Scientific, Singapore, 2007), p. 152; arXiv:nucl-th/0604043.
24. B.A. Brown, T. Duguet, T. Otsuka, D. Abe, and T. Suzuki, Phys. Rev. C **74**, 061303(R) (2006).
25. G. Colò, H. Sagawa, S. Fracasso, and P.F. Bortignon, Phys. Lett. B **646**, 227 (2007).
26. D.M. Brink and Fl. Stancu, Phys. Rev. **C75**, 064311 (2007).
27. M. Grasso, Z.Y. Ma, E. Khan, J. Margueron, and N. Van Giai, Phys. Rev. C **76**, 044319 (2007).
28. M. Zalewski, J. Dobaczewski, W. Satuła, and T.R. Werner, Phys. Rev. C **77**, 024316 (2008).
29. Wei Zhu, G. Coló, Zhongyu Ma, H. Sagawa, P.F. Bortignon, Phys. Rev. **C77**, 014314 (2007).
30. M. Kortelainen, J. Dobaczewski, K. Mizuyama, and J. Toivanen, Phys. Rev. C **77**, 064307 (2008).
31. I. Hamamoto, Phys. Lett. **61B** (1976) 343.
32. V. Bernard and N. Van Giai, Nucl. Phys. **A348**, 75 (1980).
33. E. Litvinova and P. Ring, Phys. Rev. **C73**, 044328 (2006).
34. K. Rutz, M. Bender, J.A. Maruhn, P.-G. Reinhard, W. Greiner, Nucl. Phys. **A634**, 67 (1998).
35. E. Chabanat, P. Bonche, P. Haensel, J. Meyer, and R. Schaeffer, Nucl. Phys. **A627** (1997) 710; **A635** (1998) 231.
36. P.-G. Reinhard, D.J. Dean, W. Nazarewicz, J. Dobaczewski, J.A. Maruhn, and M.R. Strayer, Phys. Rev. **C60**, 014316 (1999).

37. T. Lesinski, M. Bender, K. Bennaceur, T. Duguet, and J. Meyer, Phys. Rev. C **76**, 014312 (2007).
38. A. Oros, Ph.D. thesis, University of Köln, 1996.
39. N. Schwier, I. Wiedenhover, and A. Volya, arXiv:0709.3525.
40. M. Zalewski *et al.*, in preparation.
41. H. Flocard, Thesis 1975, Orsay, Série A, N° 1543.
42. D. Brink, Fl. Stancu, and H. Flocard, Phys. Lett. **B68**, 108 (1977).
43. M. Zalewski, W. Satuła, J. Dobaczewski, P. Olbratowski, M. Rafalski, T.R. Werner, and R.A. Wyss, arXiv:0811.0279, submitted to Eur. Phys. Jour. A.
44. G. Audi, A.H. Wapstra, and C. Thibault, Nucl. Phys. **A729**, 337 (2003).